Systems & Control Letters 204 (2025) 106218

Contents lists available at ScienceDirect

Systems & Control Letters

journal homepage: www.elsevier.com/locate/sysconle

Adaptive sampling-based event-triggered consensus for multi-agent systems

Yiming Wu [a,b], Nan Tang [a], Xiaozhen Pan [a,b,*], Ming Xu [a], Shuai Liu [c]

[a] School of Cyberspace, Hangzhou Dianzi University, Hangzhou, 310018, China
[b] Zhejiang Provincial Key Laboratory of Sensitive Data Security and Confidentiality Governance, Hangzhou, China
[c] School of Control Science and Engineering, Shandong University, Jinan, China

ARTICLE INFO

Keywords:
Event-triggered control
Multi-agent system
Consensus
Adaptive sampling mechanism

ABSTRACT

This brief addresses the event-triggered consensus problem of linear multi-agent systems (MASs) considered limited resources. A novel adaptive sampling dynamic event-triggered control (ASDETC) is proposed. It incorporates an inner self-learning term into the triggering conditions, enabling each agent to adaptively adjust its sampling detection interval based on the frequency of event triggering. To ensure effectiveness, a detection interval updating algorithm is developed. Further, we consider the adaptive sampling-based event-triggered consensus issue in directed and switching topology. With the aid of Lyapunov analysis, it is demonstrated that ASDETC can drive the MAS towards exponential consensus while effectively avoiding potential Zeno behavior. Finally, numerical simulations are conducted to validate the results.

1. Introduction

Consensus problem is of great significance for numerous algorithms and coordinated behaviors in multiagent systems (MASs), and fruitful results on consensus have been achieved over the past decades [1–3]. In most consensus algorithms, it is typically assumed that each agent utilizes continuous measurements and control signals from its neighbors to develop appropriate control protocols. However, this assumption requires substantial computational resources and an optimal communication setting for MASs, which is clearly impractical given the constraints of real-world control engineering systems such as limited bandwidth, computation, and energy resources. Therefore, a crucial consideration in designing effective consensus protocols for MASs should be ensuring good control performance while optimizing the utilization of limited resources.

Many works have investigated the possibility of reducing communication and calculation burdens caused by the continuous communication between adjacent agents or frequent updates of control inputs. For example, event-triggered control makes a great contribution in this regard. Unlike time-based intervals, the event-triggered control scheme introduces a noteworthy characteristic where the instances of selecting actions and updating controls are established according to a pre-set event triggering condition directly associated with system measurements. To address the event-triggered control problem, a variety of event-triggering mechanisms (ETMs) have been developed [4–8]. Among them, the dynamic event triggering mechanism (DETM) [9] has attracted more attention because it can dynamically adjust the triggering frequency.

Note that in most of the existing works, continuous-time event detection for DETM is required, which not only consumes a lot of communication and computation resources but also faces a difficult implementation issue for actual systems, especially for digital control systems. Ulteriorly, sampled-data control offers an alternative approach where each agent employs sampled signals in place of continuous signals from neighboring agents for the purpose of control design, where the sampling occurs after the elapse of a periodic/aperiodic time interval [10–14]. Naturally, periodic sampling detection event-triggered control (PETC) was proposed [15–18]. The PETC mechanism designed a sampler set at a fixed sampling interval to sample the state of each agent. Thus the broadcasting and examining only occur at each sampling instant. However, choosing a fixed sampling period to adapt to the various situations in the control process is a difficult thing. Therefore, aperiodic sampling detection event-triggered control (AETC) was considered in [19–22]. Based on the idea of stochastic sampling event trigger, the sliding mode control of Markovian jump systems was considered in [19]. Cheng et al. [20] provided a varying sampling static event-triggered approach while the sampling interval is bounded and determined by an event-driven strategy. A static event-triggered mechanism with aperiodic sampling to achieve consensus of fuzzy systems is proposed in [21]. Still, the determination of the sampling interval depends on extra sensors to collect the system's state data in real-time. In [22], the authors considered a nonperiodic sampling ETM by applying an upper bound ETC determined by the optimization algorithm. However, the mechanisms mentioned above are either based

* Corresponding author.
E-mail address: xzpan@hdu.edu.cn (X. Pan).

https://doi.org/10.1016/j.sysconle.2025.106218
Received 2 September 2024; Received in revised form 3 May 2025; Accepted 9 August 2025
Available online 1 September 2025

on independently different forms of stochastic sampling or require frequent acquisition of real-time states to adjust the sampling interval.

In this article, we introduce an innovative adaptive sampling dynamic event-triggering scheme (ASDETC), in which the state of per agent is sampled only at its sampling interval h_k^i. Considering that the dynamic threshold variable in DETM reflects the frequency of event triggerings, we propose integrating the sampling interval with the dynamic threshold. This combined approach allows the ASDETC to adaptively adjust the sampling interval based on the frequency of event triggerings. When event triggerings are frequent, the sampling interval is shortened, enabling more timely detection. Conversely, when event triggers are infrequent, the detection interval is prolonged to reduce unnecessary detection. By employing this approach, the ASDETC effectively improves performance and optimizes resource consumption. The sampling detection schemes among different ETMs are shown in Fig. 1. The primary advancements presented in this paper are outlined below.

1. We propose a novel event-triggered consensus protocol that differs fundamentally from previously developed methods. In our approach, the interval of event-triggered detection can adaptively scale with the frequency of triggered events. This adaptability is advantageous for both conservation of resources and convergence performance.
2. The lower bound of the required sampling interval is given to avoid the occurrence of Zeno behavior, and the relationship between the interval time and adaptive sampling detection is established explicitly.
3. An asynchronous sampling mechanism is proposed. It eliminates the need for time synchronization, which is typically difficult to achieve in large-scale MASs.
4. To verify the universality and superiority of ASDETC, adaptive sampling-based event-triggered consensus issue is investigated in directed and switching topology.

Notation: Consider a graph $\mathcal{G} = (\mathcal{V}, \mathcal{E})$ that illustrates the communication topology of a Multi-Agent System (MAS), with $\mathcal{V} = \{v_1, v_2, \dots, v_n\}$ being the set of vertices and $\mathcal{E} \subseteq \mathcal{V} \times \mathcal{V}$ representing an edge set. An edge $(v_i, v_j) \in \mathcal{E}$ signifies that vertex v_i is capable of receiving information from vertex v_j. The set of in-neighbors for vertex v_i is denoted by $\mathcal{N}_i = \{v_j \in \mathcal{V} | (v_j, v_i) \in \mathcal{E}\}$ while out-neighbors set is describes as $\mathcal{M}_i = \{v_j \in \mathcal{V} | (v_i, v_j) \in \mathcal{E}\}$. Define the adjacency matrix $\mathcal{A} = [a_{ij}]_{n\times n}$, where $a_{ii} = 0$, $a_{ij} = 1$ if node v_j is a in-neighbor of node v_i and $a_{ij} = 0$ otherwise. The Laplacian matrix is defined as $\mathcal{L} = \mathcal{D} - \mathcal{A}$, where $\mathcal{D}$ represents the in-degree matrix and $\mathcal{D} = diag\{d_1, d_2, \dots, d_n\}$, and each d_i denotes the cardinality of the in-neighbor set of the ith agent. For an undirected graph $\mathcal{G}$, $(v_i, v_j) \in \mathcal{E}$ if and only if $(v_j, v_i) \in \mathcal{E}$. $\mathbb{N}$ and $\mathbb{R}$ represent the natural number set and real number set, respectively. $\otimes$ and $\|\cdot\|$ denote the Kronecker product and the Euclidean norm, respectively.

2. Problem formulation

Contemplate a decentralized Multi-Agent System (MAS) comprising N identical agents. The behavior of these agents is characterized by the following dynamics:

$$\dot{x}_i(t) = Ax_i(t) + Bu_i(t),\ i = 1, 2, \dots, N, \tag{1}$$

where $x_i \in \mathbb{R}^n$ is the state and $u_i \in \mathbb{R}^m$ is the control input of the ith agent, respectively; $A \in \mathbb{R}^{n\times n}$ and $B \in \mathbb{R}^{n\times m}$ are the known constant matrices with appropriate dimensions. The initial condition of (1) is given by $x_i(0) = x_i^0$.

The objective of this paper is to devise an innovative event-triggered protocol ensuring that MAS (1) can achieve consensus, that is to say,

$$\lim_{t\to\infty} \left\| x_i(t) - x_j(t) \right\| = 0. \tag{2}$$

Before to proceeding, we require the following hypotheses and lemmas, which are rather conventional.

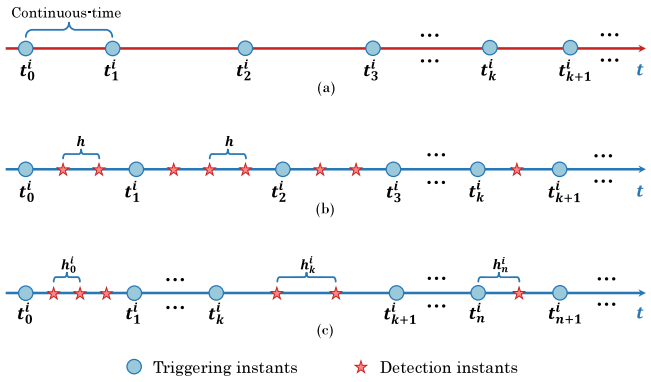

Fig. 1. (a). Continuous-time event detection. (b). Periodic sampling event detection. (c). Adaptive sampling event detection.

Assumption 1. (A, B) is stabilizable.

Assumption 2. The interaction graph $\mathcal{G}$ is assumed to be undirected and connected.

Lemma 1. *Given [23] and Assumption 1, the subsequent Algebraic Riccati Equation (ARE) possesses a solitary positive solution $P > 0$:*

$$PA + A^T P - PBB^T P + I_N = 0. \tag{3}$$

Lemma 2. *With [24] Assumption 2 in place, the eigenvalues of Laplacian matrix $\mathcal{L}$ are all real and can be arranged as follows:*

$$\omega_1 \le \omega_2 \le \cdots \le \omega_N, \tag{4}$$

in which $\omega_1 = 0$, ω_2 represents the smallest non-zero eigenvalue and ω_N denotes the largest eigenvalue of $\mathcal{L}$ respectively.

3. Main results

Inspired by [25], we first define the local consensus error:

$$z_i(t) = \sum_{j=1}^{N} a_{ij} \left(x_j(t) - x_i(t) \right). \tag{5}$$

Then, we define

$$z_i(t_k^i) = \sum_{j=1}^{N} a_{ij} \left(x_j(t_{k'}^j) - x_i(t_k^i) \right), \tag{6}$$

where $t_{k'}^j = \arg\min_{p\in\mathbb{N}} \{t - t_p^j | t \ge t_p^j\}$ for $t \in [t_k^i, t_{k+1}^i)$ and $\Gamma_i = \{t_1^i, t_2^i, \dots\}$ represents the sequences of the ith agent's triggering time instants. The measurement error of sampled data at the kth sampling is defined as

$$e_i(t) = z_i(t_k^i) - z_i(t). \tag{7}$$

We propose a state feedback control protocol for the ith agent as

$$u_i(t) = Kz_i(t_k^i), \tag{8}$$

in which K represents the gain matrix that is to be determined subsequently.

Integrating the MAS (1) with the controller (8) that has been developed, the closed-loop dynamics for the ith agent are given by the following expression:

$$\dot{x}_i(t) = Ax_i(t) + BKz_i(t_k^i),\quad t \in [t_k^i, t_{k+1}^i). \tag{9}$$

For better clarity, let $z(t) = \left[z_1^T(t), \dots, z_N^T(t)\right]^T$, $e(t) = \left[e_1^T(t), \dots, e_N^T(t)\right]^T$. In line with graph theory principles, one obtains $z(t) = -(\mathcal{L} \otimes I_n)x(t)$. Then, the resultant MAS is expressed as:

$$\dot{z}(t) = (I_N \otimes A)z(t) - (\mathcal{L} \otimes BK)z(t_k). \tag{10}$$

According to Lemmas 1 and 2, the following Riccati equation have the solution $P > 0$:

$$PA + A^T P - PBRB^T P + I_N = 0, \tag{11}$$

where $R^{-1} = \lambda\omega_2$ with $\lambda > 0$ being a parameter to be designed.

To integrate adaptive sampling detection into our triggering mechanism, we introduce h_k^i as the sampling period for the ith agent between the kth and $(k+1)th$ triggering instants, which means the interval is a multiple of h_k^i, denoted by $l_i h_k^i, (l_i = 1, 2, \ldots)$, $t_{k+1}^i = t_k^i + l_i h_k^i$. We will present the algorithm for determining h_k^i later. For the sake of simplicity, denote $t_s^i = t_k^i + l_i h_k^i$. The event trigger protocol is given as follows

$$\begin{cases} t_{k+1}^i = \inf\left\{ t_s^i > t_k^i \,|\, \|e_i(t_s^i)\|_{\Phi}^2 - \beta_i \left\|z_i(t_k^i)\right\|_{\Phi}^2 - \gamma_i \eta_i(t_s^i) > 0 \right\} \\ \dot{\eta}_i(t) = -\alpha_i \eta_i(t) + \theta_i \left(\beta_i \left\|z_i(t_k^i)\right\|_{\Phi}^2 - \|e_i(t_s^i)\|_{\Phi}^2 \right), \eta_i(0) > 0. \end{cases} \tag{12}$$

Here, we define $\|e_i(t_s^i)\|_{\Phi}^2$ as $e_i^T(t_s^i)\Phi e_i(t_s^i)$ and $\left\|z_i(t_k^i)\right\|_{\Phi}^2$ as $z_i^T(t_k^i)\Phi z_i(t_k^i)$, where Φ represents a positive definite weighted matrix that will be designed later. Additionally, we assume that $\alpha_i > 0$, $\beta_i > 0$, and $\gamma_i > 0$. We introduce $\eta_i(t)$ as a positive time-dependent variable, where $\eta_i(0)$ serves as the initial dynamic threshold. It is crucial to recognize that the local consensus deviation $z_i(t)$ will asymptotically approach 0 as the system achieves consensus.

From (12), one can see that as an important component of the event triggering protocol, the dynamic threshold $\eta_i(t)$ is influenced by the difference between local consensus error $z_i(t_k^i)$ and the measurement errors $e_i(t_s^i)$ and can be intuitively regarded as a filtered value of difference between the two errors. The dynamic threshold adjusts the trigger frequency through a self-learning mechanism. A rapid increase in the dynamic threshold suggests that the triggering frequency is excessively high and necessitates urgent restriction by elevating the threshold. Conversely, a swift decrease indicates that the triggering frequency is too low and requires enhancement by lowering the threshold. Given these characteristics, we incorporate this mechanism into adjusting sampling detection intervals to enable adaptive changes in detection intervals.

As mentioned above, For the self-learning term $\boldsymbol{\eta_i(t)}$, that is, the dynamic threshold, it can be intuitively regarded as a filtered value of the errors, and its variation can be used to reflect the triggering frequency. Specifically, as we can see from the Eq. (12), $\boldsymbol{\eta_i(t)}$ evolves along with the difference value between the errors of the designed triggering mechanism. When the difference value becomes bigger, the change rate of $\boldsymbol{\eta_i(t)}$ varies adaptively to increase the value of $\boldsymbol{\eta_i(t)}$. Thus, the increasing part of the difference value will be countered. The same counteraction is obvious when the exceeding value becomes smaller. It is precisely through the variation of the self-learning term $\boldsymbol{\eta_i(t)}$ that we can obtain information about the current frequency of event triggering and thus increase or decrease the interval time.

Remark 1. In contrast to continuous event-triggered detection, the sampling strategy proposed in this brief offers two advantages: (1) for the ith agent, the strategy relies solely on the sampled data $x_j(t_s^i)$ from the neighboring agents that are broadcasted, rather than utilizing the continuous state $x_j(t)$; and (2) the event-triggered condition needs to be checked only at each sampling instance, indicating that there is no requirement for additional hardware to support continuous measurement and computation.

Now, we will introduce the Adaptive Sampling Detection (ASD) algorithm. By means of this algorithm, an agent is enabled to acquire its individual sampling interval for the subsequent triggering event. For the ith agent, let h_m and h_M represent the lower and upper bounds of the sampling detection interval, respectively, such that $h_m \le h_k^i \le h_M$. We define t_d^i as the latest detection instant and η_i' as the most recent triggered value of $\eta_i(t_k^i)$. The pseudocode of ASD is presented in Algorithm 1.

Algorithm 1 ASD.

Require: Set $h_m, h_k^i, h_M, 0 < h_m < h_k^i < h_M, h_0^i = \frac{h_m + h_M}{2}, \delta = h_M - h_m, t_d^i = 0, t_0^i = 0, \eta_i' = \eta_i(0) > 0$;

```
while t < T, T denotes the intended operational duration of the system do
  if t − t_d^i > h_k^i then
    perform detection;
    if the event-triggering condition is met, then
      Update h_k^i = h_0^i + δ×atan((η_i(t)−η_i')/(t−t_{k−1}^i))/π, η_i' = η_i(t) and t_k^i = t;
      Consider that h_m < h_k^i < h_M, set h_k^i = h_M if h_k^i > h_M and h_k^i = h_m if h_k^i < h_m;
    end if
    Update t_d^i = t;
  end if
end while
```

Remark 2. Note that if $h_m = h_M$, then the h_k^i will be a constant h_0^i, which means the sampling mechanism is periodic.

Remark 3. It is worth mentioning that under Algorithm 1, we guarantee the equal detection interval h_k^i between two consecutive triggering instants and allow it to rise and fall between triggering intervals based on a fixed value h_0^i, which means our detection is periodic between two adjacent triggering points but aperiodic for the entire process. The update of the detection interval only occurs with one triggering, which avoids unnecessary resource waste for changing the interval.

Remark 4. In our proposed ASDETC, the determination of the sampling interval h_k^i for each the ith agent is based on the dynamic threshold parameter η_i and the triggering instant t_k^i. As a consequence, agents operate with distinct sampling intervals, resulting in an asynchronous sampling scheme. In contrast to the periodic dynamic event-triggered control (PDETC) scheme, where all agents uniformly adopt the same sampling interval, leading to pronounced difficulties in synchronizing the sampling periods, our approach effectively surmounts the synchronization challenges and has long plagued large-scale distributed networks. The existing aperiodic sampling schemes rely on constantly monitoring the system's real-time state to adjust the sampling interval. Our ASD algorithm only requires information from within the agent. This means that as the number of nodes scales up, our algorithm remains efficient.

Theorem 1. *Under Assumptions 1 and 2, let $K = \lambda B^T P$ and $\Phi = PBB^T P$, where $P > 0$ is the solution of (11). Then, the MAS (1) can reach consensus under the event-triggered scheme (12) if the parameters satisfy*

$$\lambda\omega_N c^2 + \max\{\theta_i\beta_i\} \le \lambda\omega_2, \tag{13}$$

where $c = (\|A\| + \lambda\|\mathcal{L} \otimes BB^T P\|)h_M$, and

$$\lambda\omega_N \le \min\{\theta_i\}. \tag{14}$$

Proof. Over the interval $t \in \left[t_k^i, t_{k+1}^i\right)$, for the ith agent, as per Equation (12), it is evident that the triggering condition remains unmet. Thereafter, we obtain the following: $\|e_i(t_s^i)\|_{\Phi}^2 - \beta_i \left\|z_i(t_k^i)\right\|_{\Phi}^2 \le \gamma_i \eta_i(t_s^i)$. Take into account the following mixed Lyapunov function:

$$W(t) = V(t) + \sum_{i=1}^{n} \eta_i(t), \tag{15}$$

where $V(t) = z^T(t)(I_N \otimes P)z(t) \ge 0$. In fact, solving the differential equation from (12), yields:

$$\eta_i(t) = e^{-\alpha_i(t-t_s^i)}\eta_i(t_s^i) + \frac{1}{\alpha_i}\left(1 - e^{-\alpha_i(t-t_s^i)}\right)$$

$$\theta_i(\beta_i \left\| z_i(t_k^i) \right\|_{\Phi}^2 - \left\| e_i(t_s^i) \right\|_{\Phi}^2). \tag{16}$$

Noted that Eq. (16) is formulated to describe the dynamic threshold $\eta_i(t)$ by solving the differential Equation (12) and establishing a relationship between the continuous terms and discrete terms of the dynamic threshold.

For $t \in \left[t_k^i, t_{k+1}^i\right)$, one has

$$-\gamma_i \eta_i(t_s^i) \le \beta_i \left\| z_i(t_k^i) \right\|_{\Phi}^2 - \left\| e_i(t_s^i) \right\|_{\Phi}^2. \tag{17}$$

Then, we have

$$\begin{aligned}
\eta_i(t) &\ge e^{-\alpha_i(t-t_s^i)}\eta_i(t_s^i) + \frac{1}{\alpha_i}(e^{-\alpha_i(t-t_s^i)} - 1)\theta_i\gamma_i\eta_i(t_s^i) \\
&= \frac{\theta_i\gamma_i}{\alpha_i}\left((\frac{\alpha_i}{\theta_i\gamma_i} + 1)e^{-\alpha_i(t-t_s^i)} - 1\right)\eta_i(t_s^i) \\
&\ge \frac{\theta_i\gamma_i}{\alpha_i}\left((\frac{\alpha_i}{\theta_i\gamma_i} + 1)e^{-\alpha_i h_k^i} - 1\right)\eta_i(t_s^i) \\
&\ge \frac{\theta_i\gamma_i}{\alpha_i}\left((\frac{\alpha_i}{\theta_i\gamma_i} + 1)e^{-\alpha_i h_k^i} - 1\right)\Lambda\eta_i(0),
\end{aligned} \tag{18}$$

where $\Lambda \ge 0$. By selecting $(\frac{\alpha_i}{\theta_i\gamma_i} + 1)e^{-\alpha_i h_k^i} \ge 1$, it is established that $0 < h_k^i \le \dfrac{\ln(\frac{\alpha_i}{\theta_i\gamma_i} + 1)}{\alpha_i}$. Taking into consideration the range $h_m \le h_k^i \le h_M$, it suffices to ensure that $0 < h_M \le \dfrac{\ln(\frac{\alpha_i}{\theta_i\gamma_i} + 1)}{\alpha_i}$. Consequently, we deduce that $\eta_i(t) \ge 0$ for all $t > 0$.

Since $V(t) > 0$ and $\eta_i(t) > 0$, we obtain $W(t) > 0$. For $t \in \left[t_k^i, t_{k+1}^i\right)$, $\dot{V}(t)$ is easily to obtain:

$$\begin{aligned}
\dot{V}(t) &= \dot{z}^T(t)(I_N \otimes P)z(t) + z^T(t)(I_N \otimes P)\dot{z}(t) \\
&= z^T(t)(I_N \otimes (A^TP + PA))z(t) - z^T(t_k)(\mathcal{L} \otimes PBK)^T z(t) \\
&\quad - z^T(t)(\mathcal{L} \otimes PBK)z^T(t_k).
\end{aligned} \tag{19}$$

The property of the undirected graph $\mathcal{G}$ yields $\mathcal{L}^T = \mathcal{L}$ and the condition $K = \lambda B^T P$ suggests that $PBK = (PBK)^T = \lambda\Phi$. Subsequently, the deduction can be made by applying the square completion process to the non-quadratic part in Eq. (19).

$$\begin{aligned}
\dot{V}(t) &= z^T(t)(I_N \otimes (A^TP + PA))z(t) - \lambda\left[z^T(t_k)(\mathcal{L} \otimes \Phi)z(t) + z^T(t)(\mathcal{L} \otimes \Phi)z(t_k)\right] \\
&= z^T(t)(I_N \otimes (A^TP + PA))z(t) - \lambda\left[z^T(t_k)(\mathcal{L} \otimes \Phi)z(t_k) + z^T(t)(\mathcal{L} \otimes \Phi)z(t)\right. \\
&\quad \left. - (z(t_k) - z(t))^T(\mathcal{L} \otimes \Phi)(z(t_k) - z(t))\right].
\end{aligned} \tag{20}$$

By Lemma 2, we obtain $\omega_2 z^T(t)(I_N \otimes \Phi)z(t) \le z^T(t)(\mathcal{L} \otimes \Phi)z(t) \le \omega_N z^T(t)(I_N \otimes \Phi)z(t)$. Then, we have

$$\begin{aligned}
\dot{V}(t) &\le z^T(t)(I_N \otimes (A^TP + PA - PBRB^TP))z(t) - \lambda z^T(t_k)(\mathcal{L} \otimes \Phi)z(t_k) \\
&\quad + \lambda(z(t_k) - z(t_s))^T(\mathcal{L} \otimes \Phi)(z(t_k) - z(t_s)) \\
&\quad + \lambda(z(t_s) - z(t))^T(\mathcal{L} \otimes \Phi)(z(t_s) - z(t)) \\
&\le -\sum_{i=1}^N z_i^T(t)z_i(t) - \lambda\omega_2\sum_{i=1}^N \left\| z_i(t_k^i) \right\|_{\Phi}^2 + \lambda\omega_N\sum_{i=1}^N \left\| e_i(t_s^i) \right\|_{\Phi}^2 \\
&\quad + \lambda\omega_N(z(t_s) - z(t))^T(I_N \otimes \Phi)(z(t_s) - z(t)).
\end{aligned} \tag{21}$$

For the part $(z(t_s) - z(t))^T(I_N \otimes \Phi)(z(t_s) - z(t))$, note that $t - t_s \le h_M$ for any $s \in \mathbb{N}$. Then, for any $t \in [t_s, t_{s+1}]$,

$$\|z(t_s) - z(t)\| \le \int_{t_s}^t \|\dot{z}(\tau)\| d\tau \le h_M \|\dot{z}(\tau)\|_M. \tag{22}$$

where $\|\dot{z}(\tau)\|_M = \max_{\tau\in[t,t_s]} \|\dot{z}(\tau)\|$, Due to the fact that $z(t)$ represents the local consensus error, based (10), it follows that

$$\begin{aligned}
\|\dot{z}(t)\| &= \|(I_N \otimes A)z(t) - (\mathcal{L} \otimes BK)z(t_k)\| \\
&\le \|A\|\|z(t)\| + \lambda\|\mathcal{L} \otimes BB^TR\|\|z(t_k)\|
\end{aligned} \tag{23}$$

Case 1: If $\|z(t)\| > |\|z(t_k)\||$, which leads to

$$\begin{aligned}
\|z(t_s) - z(t)\| &\le h_M(\|A| + \lambda\|\mathcal{L} \otimes BB^TR\|)\|z(t)\| \\
&= c\|z(t)\|.
\end{aligned} \tag{24}$$

This further implies,

$$\begin{aligned}
\lambda\omega_N(z(t_s) - z(t))^T(I_N \otimes \Phi)(z(t_s) - z(t)) &\le \lambda\omega_N c^2 \sum_{i=1}^N \left\| z_i(t) \right\|_{\Phi}^2 \\
&\le \lambda\omega_N\lambda_{max}(\Phi)c^2\sum_{i=1}^N z_i^T(t)z_i(t).
\end{aligned} \tag{25}$$

Given that (13) and (14) are satisfied, combining (21) and (25), we have

$$\begin{aligned}
\dot{W}_s(t) &= \dot{V}(t) + \sum_{i=1}^N \dot{\eta}_i(t) \\
&\le (\lambda\omega_N\lambda_{max}(\Phi)c^2 - 1)\sum_{i=1}^N z_i^T(t)z_i(t) - \sum_{i=1}^N \alpha_i\eta_i(t) \\
&\quad + \sum_{i=1}^N \left((\theta_i\beta_i - \lambda\omega_2)\left\| z_i(t_k^i) \right\|_{\Phi}^2 \right. \\
&\quad \left. - (\theta_i - \lambda\omega_N)\left\| e_i(t_s^i) \right\|_{\Phi}^2\right) \\
&\le (\lambda\omega_N\lambda_{max}(\Phi)c^2 - 1)\sum_{i=1}^N z_i^T(t)z_i(t) - \sum_{i=1}^N \alpha_i\eta_i(t).
\end{aligned} \tag{26}$$

Case 2: $\|z(t)\| \le |\|z(t_k)\||$, then conclusion will be

$$\begin{aligned}
\dot{W}_s(t) &\le -\sum_{i=1}^N z_i^T(t)z_i(t) - \sum_{i=1}^N \alpha_i\eta_i(t) \\
&\quad + \sum_{i=1}^N \left((\theta_i\beta_i + \lambda\omega_N c^2 - \lambda\omega_2)\left\| z(t_k^i) \right\|_{\Phi}^2 \right. \\
&\quad \left. - (\theta_i - \lambda\omega_N)\left\| e_i(t_s^i) \right\|_{\Phi}^2\right) \\
&\le -\sum_{i=1}^N z_i^T(t)z_i(t) - \sum_{i=1}^N \alpha_i\eta_i(t).
\end{aligned} \tag{27}$$

To enhance the conservativeness of the MASs to a greater extent, we have

$$\dot{W}(t) \le -\sum_{i=1}^N z_i^T(t)z_i(t) - \sum_{i=1}^N \alpha_i\eta_i(t). \tag{28}$$

Given the definition of $W(t)$, it can be verified that $W(t) \le \lambda_{max}(P)\sum_{i=1}^N \left\| z_i(t) \right\|^2 + \sum_{i=1}^N \eta_i(t)$. So, it is inferred that

$$\dot{W}(t) \le -\varsigma W(t), \tag{29}$$

where $\varsigma = \min(\frac{1}{\lambda_{max}(P)}, \min\{\alpha_i, i \in \mathcal{V}\})$. Hence, we arrive at the following results:

$$W(t) \le e^{-\varsigma t}W(0), \tag{30}$$

This signifies that the Multi-Agent System (MAS) described by Eq. (1) reaches consensus with an exponential convergence rate of ς.

It should be noted that although global information is employed in the theoretical proof, this does not undermine the distributed nature of the algorithm. The eigenvalues ω_2 and ω_N can be regarded as a signal for quantifying the network's connectivity characteristics. Meanwhile, the solution P of the Riccati equation serves as a theoretical construct for designing control laws and analyzing system stability. The key to a fully distributed algorithm lies in how agents make decisions and exchange information. Our algorithm is designed to be distributed in terms of agent-level decision-making and communication. Agents in our system only use local information to determine their control actions and trigger events, which aligns with the concept of fully distributed.

The abovementioned discussion has focused on undirected networks. Next, we will extend the scope of our study to directed and switching topologies networks. The switching signal of the graph is

described as $\sigma \in \{1, 2, \dots, M\}$, where M denotes the maximum number of possible topologies. Here we use $\mathcal{L}^\sigma$ to replace the Laplacian matrix $\mathcal{L}$ defined in the above. Before the formal theorem, we first present the following assumptions and lemmas.

Assumption 3. The directed graph $\mathcal{G}^\sigma$ is assumed to be strongly connected.

Lemma 3. *Given [26] and Assumption 3, for a strongly connected network $\mathcal{G}^\sigma$ with Laplacian matrix $\mathcal{L}^\sigma$, there will exist a vector with all the elements to be positive $\zeta^\sigma = \{\zeta_1^\sigma, \zeta_2^\sigma, \dots \zeta_N^\sigma\}^T$ so that $\zeta^{\sigma T}\mathcal{L}^\sigma = 0$ and $\sum_{i=1}^N \zeta_i^\sigma = 1$. Let H^σ represent the diagonal matrix from ζ_1^σ to ζ_N^σ. Then $\tilde{\mathcal{L}}^\sigma = (H^\sigma\mathcal{L}^\sigma + \mathcal{L}^{\sigma T}H^\sigma)/2$ is a symmetric matrix with all the eigenvalues are non-negative. Let $\tilde{\omega}_2^\sigma$ represents the smallest non-zero eigenvalue and $\tilde{\omega}_N^\sigma$ denotes the largest eigenvalue of $\tilde{\mathcal{L}}^\sigma$ respectively.*

Lemma 4. *Given [27] and Assumption 3, the general algebraic connectivity for a strongly connected graph is defined by*

$$a(\mathcal{L}^\sigma) = \min_{x^T\zeta=0, x\neq 0} \frac{x^T\tilde{\mathcal{L}}^\sigma x}{x^T H^\sigma x}. \tag{31}$$

Similar with (11), based on Lemmas 1 and 4, the following Riccati equation have a solution $P > 0$ with $R^{-1} = 2\lambda a(\mathcal{L}^\sigma)$.

Theorem 2. *Under Assumptions 1 and 3, let $K = \lambda B^T P$ and $\Phi = PBB^T P$. Then, the MAS (1) can reach consensus under the event-triggered scheme (12) if the parameters satisfy*

$$\lambda\tilde{\omega}_N^\sigma c^2 + \max\{\theta_i\beta_i\} \le \lambda\tilde{\omega}_2^\sigma, \tag{32}$$

where $c = (\|A\| + \lambda\|\tilde{\mathcal{L}}^\sigma \otimes BB^T P\|)h_M$, and

$$\lambda\tilde{\omega}_N^\sigma \le \min\{\theta_i\}. \tag{33}$$

Proof. Over the interval $t \in \left[t_k^i, t_{k+1}^i\right)$, consider the following mixed Lyapunov function:

$$W(t) = V(t) + \sum_{i=1}^n \eta_i(t), \tag{34}$$

where $V(t) = z(t)^T(H^\sigma \otimes P)z(t)$. It is clear that $V(t) > 0$ and $\eta_i(t) > 0$ such that $W(t) > 0$.

$$\begin{aligned}
\dot{V}(t) &= z^T(t)(H^\sigma \otimes (A^T P + PA))z(t) - \lambda\big[z^T(t_k)(\tilde{\mathcal{L}}^\sigma \otimes \Phi)z(t_k) + z^T(t)(\tilde{\mathcal{L}}^\sigma \otimes \Phi)z(t) \\
&\quad - (z(t_k) - z(t))^T(\tilde{\mathcal{L}}^\sigma \otimes \Phi)(z(t_k) - z(t))\big] \\
&\le z^T(t)(H^\sigma \otimes (A^T P + PA - 2\lambda a(\mathcal{L}^\sigma)\Phi))z(t) - \lambda z^T(t_k)(\tilde{\mathcal{L}}^\sigma \otimes \Phi)z(t_k) \\
&\quad + (z(t_k) - z(t))^T(\tilde{\mathcal{L}}^\sigma \otimes \Phi)(z(t_k) - z(t)) \\
&\le -\sum_{i=1}^N \zeta_i z_i^T(t)z_i(t) - \lambda\tilde{\omega}_2^\sigma \sum_{i=1}^N \left\|z_i(t_k^i)\right\|_\Phi^2 + \lambda\tilde{\omega}_N^\sigma \sum_{i=1}^N \left\|e_i(t_s^i)\right\|_\Phi^2 \\
&\quad + \lambda\tilde{\omega}_N^\sigma (z(t_s) - z(t))^T(I_N \otimes \Phi)(z(t_s) - z(t)).
\end{aligned} \tag{35}$$

Similar with Theorem 1, one derives

$$\begin{aligned}
\dot{W}(t) &\le -\sum_{i=1}^N \zeta_i z_i^T(t)z_i(t) - \sum_{i=1}^N \alpha_i\eta_i(t) \\
&\le -\varsigma W(t),
\end{aligned} \tag{36}$$

which conduct the same result as (29). This completes the proof.

4. Simulation results

In this section, we examine the application of spacecraft formation flight as a case study to demonstrate the efficacy of the theoretical outcome presented. The Multi-Agent System (MAS) under consideration comprises six agents and operates in a three-dimensional space. The kinematic equations governing the motion of each individual agent are formulated as follows:

$$m_i\begin{pmatrix}\ddot{X}_i\\ \ddot{Y}_i\\ \ddot{Z}_i\end{pmatrix} = \begin{pmatrix}0\\0\\m_i g\end{pmatrix} + T\begin{pmatrix}0\\0\\-F_i\end{pmatrix}$$

Here, $\ddot{X}_i$, $\ddot{Y}_i$, and $\ddot{Z}_i$ represent the accelerations of the ith agent along the X, Y, and Z axes respectively within the global coordinate system. The parameter m_i denotes the mass of the ith agent, g stands for the gravitational acceleration, F_i represents the resultant external force acting on the agent, and the matrix T serves as the transformation matrix that maps vectors from the body-fixed coordinate system of the agent to the global world coordinate system.

To facilitate the analysis and control design, we define the state vector $x_i(t)$ of the ith agent to comprehensively capture both the position and velocity information. Specifically,

$$x_i(t) = \begin{pmatrix}p_{xi}(t) & p_{yi}(t) & p_{zi}(t) & v_{xi}(t) & v_{yi}(t) & v_{zi}(t)\end{pmatrix}^T$$

where $p_{xi}(t)$, $p_{yi}(t)$, and $p_{zi}(t)$ denote the positions of the agent along the X, Y, and Z axes, and $v_{xi}(t)$, $v_{yi}(t)$, and $v_{zi}(t)$ represent the corresponding velocities.

The control input vector $u_i(t)$ is introduced to manipulate the motion of the agent and is defined as:

$$u_i(t) = \begin{pmatrix}u_{xi}(t) & u_{yi}(t) & u_{zi}(t)\end{pmatrix}^T$$

By reformulating the kinematic equations into a system of first-order differential equations, we can effectively transform them into a standard state-space representation.

$$\dot{x}_i(t) = Ax_i(t) + Bu_i(t),\ i = 1, 2, \dots, N, \tag{37}$$

with $A = \begin{pmatrix}0 & I_3\\ A_1 & A_2\end{pmatrix}$, $B = \begin{pmatrix}0\\I_3\end{pmatrix}$, $A_1 = \begin{pmatrix}0 & 0 & 0\\ 0 & 3\psi_0^2 & 0\\ 0 & 0 & -\psi_0^2\end{pmatrix}$, $A_2 = \begin{pmatrix}0 & 2\psi_0 & 0\\ -2\psi_0 & 0 & 0\\ 0 & 0 & 0\end{pmatrix}$, where $\psi_0 = 0.001$.

Example I: The undirected network topology of MASs is shown in Fig. 2. It can be confirmed that Assumptions 1 and 2 are met in this instance, consequently fulfilling all the prerequisites of Theorem 1. According to Lemma 2, it is obtained that the smallest nonzero eigenvalue $\omega_2 = 1.3819$ while the largest eigenvalue $\omega_N = 6.00$. Solving the ARE (11) with the parameter R set to 1, yields that $\lambda = 0.7236$ and $K = \begin{pmatrix}\psi_1 & \psi_2 & 0 & \psi_3 & 0 & 0\\ -\psi_2 & \psi_1 & 0 & 0 & \psi_3 & 0\\ 0 & 0 & \psi_1 & 0 & 0 & \psi_3\end{pmatrix}$, where $\psi_1 = 0.7236, \psi_2 = -0.0008, \psi_3 = 1.2533$.

The other parameters are given as $\beta_i = \begin{pmatrix}2.8 & 1.2 & 1.2 & 2.4 & 2.0 & 1.6\end{pmatrix}\times 10^{-3}$, $\eta_i(0) = \begin{pmatrix}2 & 2 & 2 & 2 & 2 & 2\end{pmatrix}$, $\theta_i = 80$, $\alpha_i = 0.004$, $\gamma_i = 0.002$, $h_m = 0.02s$, $h_M = 0.04s \le (\ln(\frac{\alpha_i}{\theta_i\gamma_i} + 1))/\alpha_i = 6.1732$, $h_0^i = 0.03s$, $\lambda\omega_N c^2 + \max\{\theta_i\beta_i\} = 0.8753 < \lambda\omega_2 = 1$, $\lambda\omega_N = 4.3416 < \theta_i$. With randomly chosen initial conditions, we carry out a series of simulations using MATLAB. The triggering instants of the ASDETC are depicted in Fig. 3(a) and it is clearly shown that under our protocol no Zeno behavior appears.

Figs. 3(b) and 4(a) illustrate the progression of agents' position and velocity states as governed by the suggested event-triggered consensus algorithm. As anticipated, the velocities of all agents converge to a common value on all three dimensions. The trajectories of the agents asymptotically approach the same path, indicating the successful achievement of consensus in the MAS.

The dynamic threshold η_i for each agent is recorded and visualized in Fig. 4(b). The plot illustrates the variation of η_i, depicting an initial increase followed by a decrease, until it eventually converges towards 0. Fig. 5 illustrates the evolution of the adaptive detection interval of each agent on the interval [0, 60s).

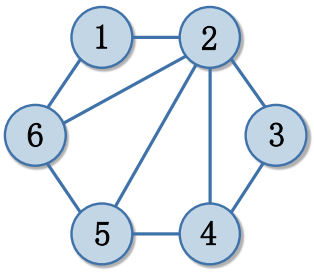

$$\mathcal{A} = \begin{pmatrix} 0 & 1 & 0 & 0 & 0 & 1 \\ 1 & 0 & 1 & 1 & 0 & 1 \\ 0 & 1 & 0 & 1 & 0 & 0 \\ 0 & 1 & 1 & 0 & 1 & 0 \\ 0 & 1 & 0 & 1 & 0 & 1 \\ 1 & 1 & 0 & 0 & 1 & 0 \end{pmatrix}$$

Fig. 2. The interaction topology among 6 agents and its adjacency matrix $\mathcal{A}$.

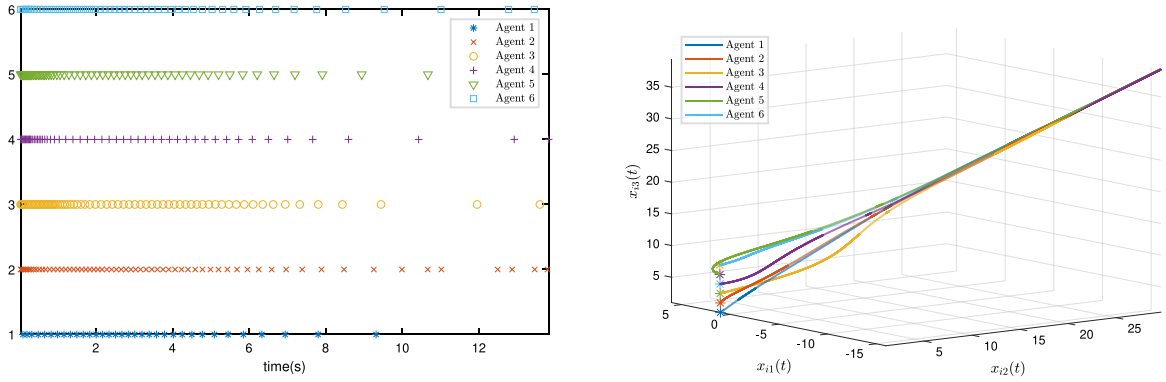

(a) (b)

Fig. 3. (a). Triggering instants of each agent under ASDETC algorithm of Example I. (b). Trajectory curves of agents' position state of Example I.

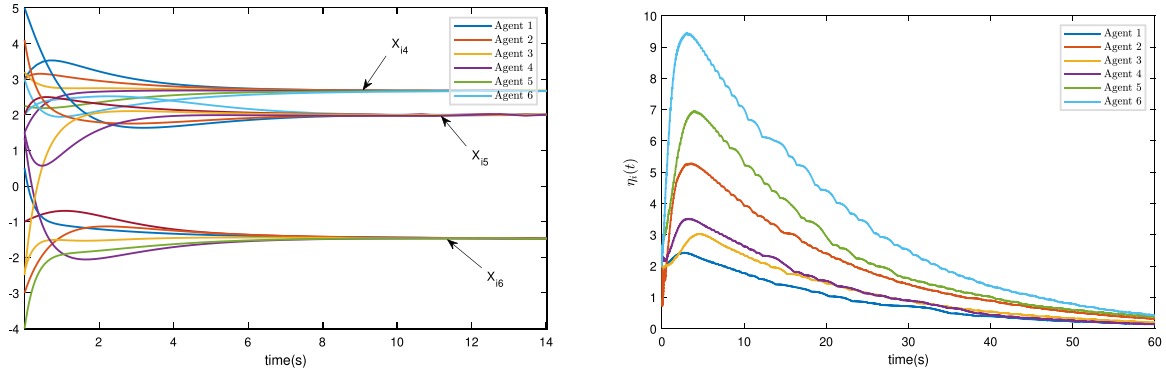

(a) (b)

Fig. 4. (a). Trajectory curves of agents' velocity state of Example I. (b). Trajectory curve of the threshold value η_i for each agent of Example I.

Table 1
The comparative analysis of triggering counts among agents.

Agents	Agent 1	Agent 2	Agent 3	Agent 4	Agent 5	Agent 6	Total
ASDETC	34	64	71	56	62	56	343
PDETC	36	82	77	70	76	68	477

By setting $h_M = h_m = 0.03s$, we can obtain the PDETC. Keeping the same experimental conditions and comparing the result of two protocols, the convergence time under the average standard deviations of six states $\bar{e} < 0.005$ of ASDETC is 14.0100s while that of PDETC is 25.9260s, which can be concluded that ADETC has better convergence performance. The numbers of triggering and detection are displayed in Table 1 and Table 2 respectively.

In comparison to the PDETC scheme, the ASDETC scheme proposed in this study exhibits fewer triggerings and detection numbers, indicating that our protocol achieves superior energy-saving performance.

Example II: Consider a MASs also composed of 6 agents. Its topological structure is shown as Fig. 6 and it will randomly change between two topological structures $\mathcal{G}^1$ and $\mathcal{G}^2$. The system matrices A and B are consistent with those in Experiment 1. It can be seen that Assumption 1 and Assumption 3 are satisfied in this instance. Based on Lemma 3, we can obtain that $\tilde{\omega}_2^1 = 0.1044$, $\tilde{\omega}_N^1 = 0.8770$, $\tilde{\omega}_2^2 = 0.1116$, $\tilde{\omega}_N^2 = 0.8237$ Based on Lemma 4, we can get $a(\mathcal{L}^1) = 0.8329$ and $a(\mathcal{L}^2) = 0.6755$. By setting $R = 1$ and solving the Riccati equation, we can obtain $\lambda = 1.1201$ for $\mathcal{G}^1$ and $\lambda = 1.4804$ for $\mathcal{G}^2$ respectively.

The other parameters are set as follows.

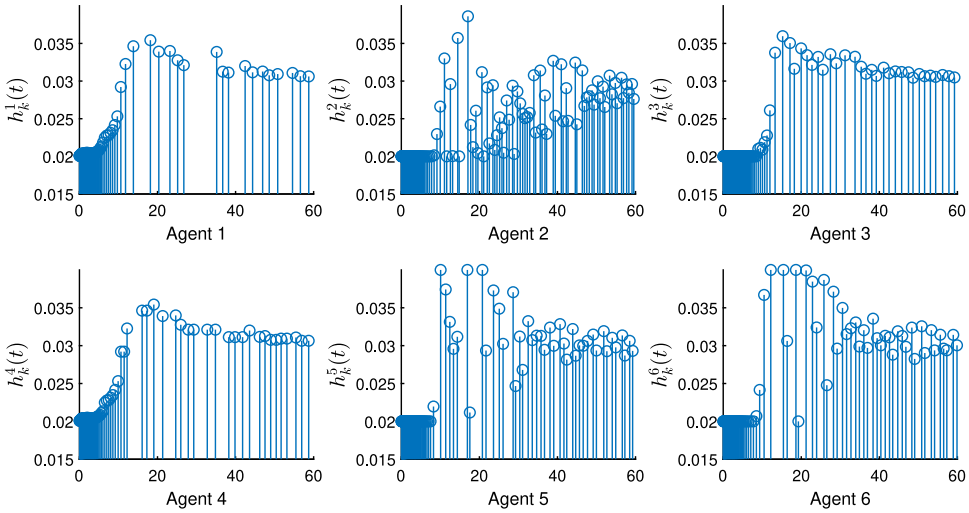

Fig. 5. Time evolutions of detection interval of each agent of Example I.

Table 2
The comparative analysis of detection counts among agents.

Agents	Agent 1	Agent 2	Agent 3	Agent 4	Agent 5	Agent 6	Total
ASDETC	544	657	572	557	552	576	3458
PDETC	860	860	860	860	860	860	5160

Table 3
The performance comparison with different detection interval.

	h_m(s)	h_M(s)	h_0^i(s)	Triggering numbers	Detection numbers	Convergence time (s)
Case1	0.015	0.045	0.03	469	7622	22.0020
Case2	0.02	0.04	0.03	425	5507	20.9430
Case3	0.025	0.035	0.03	290	2593	**11.9430**
Case4	0.01	0.03	0.02	570	13902	30.6720
Case5	0.015	0.025	0.02	414	5438	20.3850

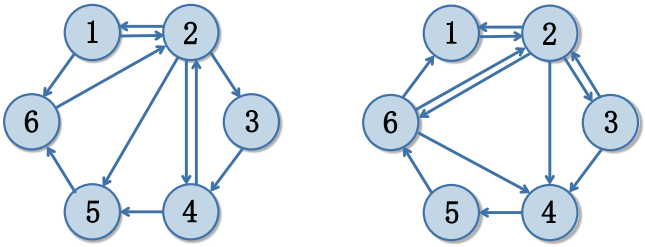

Fig. 6. The switch interaction topology among 6 agents of Example II.

$\beta_i = \begin{pmatrix}1.4 & 1.6 & 1.2 & 1.4 & 1.6 & 1.6\end{pmatrix} \times 10^{-3}$,
$\eta_i(0) = \begin{pmatrix}2 & 7 & 3 & 4 & 3 & 5\end{pmatrix}$, $\theta_i = 50$, $\alpha_i = 0.004$, $\gamma_i = 0.004$, $h_m = 0.025s$, $h_M = 0.035s \leq (\ln(\frac{\alpha_i}{\theta_i\gamma_i}+1))/\alpha_i = 0.4995$, $h_0^i = 0.03s$, $\lambda\tilde{\omega}_N^1 c^2 + \max\{\theta_i\beta_i\} = 0.0924 < \lambda\tilde{\omega}_2^1 = 0.1253$, $\lambda\tilde{\omega}_N^2 c^2 + \max\{\theta_i\beta_i\} = 0.0907 < \lambda\tilde{\omega}_2^2 = 0.1340$, $\lambda\omega_N^1 = 0.9823 < \lambda\omega_N^2 = 1.2194 < \theta_i$.

By setting the same consensus threshold $\bar{e} < 0.005$, Fig. 7 depict the triggering instants of the ASDETC and it is evident from the figure that Zeno behavior is not manifested in the directed switching topologies system under our protocol. According to Fig. 8, it indicates that the trajectories of the agents can asymptotically meet the same state, which can be deduced that consensus is achieved in the MASs.

Furthermore, in order to provide a comparison of the convergence performance under different resource utilization rates, while ensuring the convergence consensus with the previous content, we conducted multiple sets of experiments with different detection intervals. The

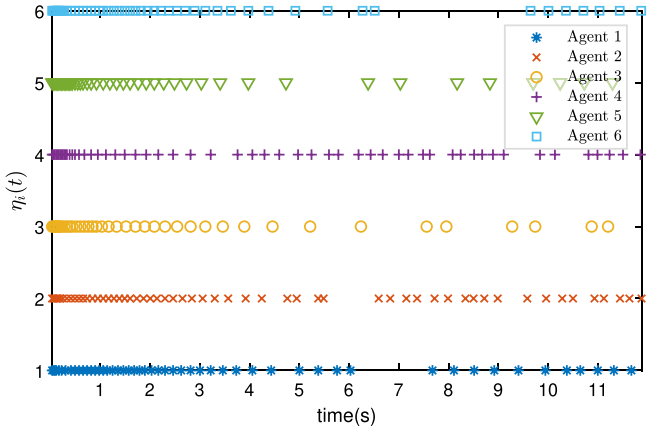

Fig. 7. Triggering instants of each agent under ASDETC algorithm of Example II.

total triggering numbers, detection numbers, and convergence time are recorded in Table 3, respectively.

Example III: Consider a MAS composed of 20 agents and the state of each agent can be described as $x_i = (x_{i1}, x_{i2}, x_{i3})$. The topological structure is shown as Fig. 9, According to Lemma 2, we can obtain that $\omega_2 = 1.5459$ while the largest eigenvalue $\omega_N = 10.6234$. The system

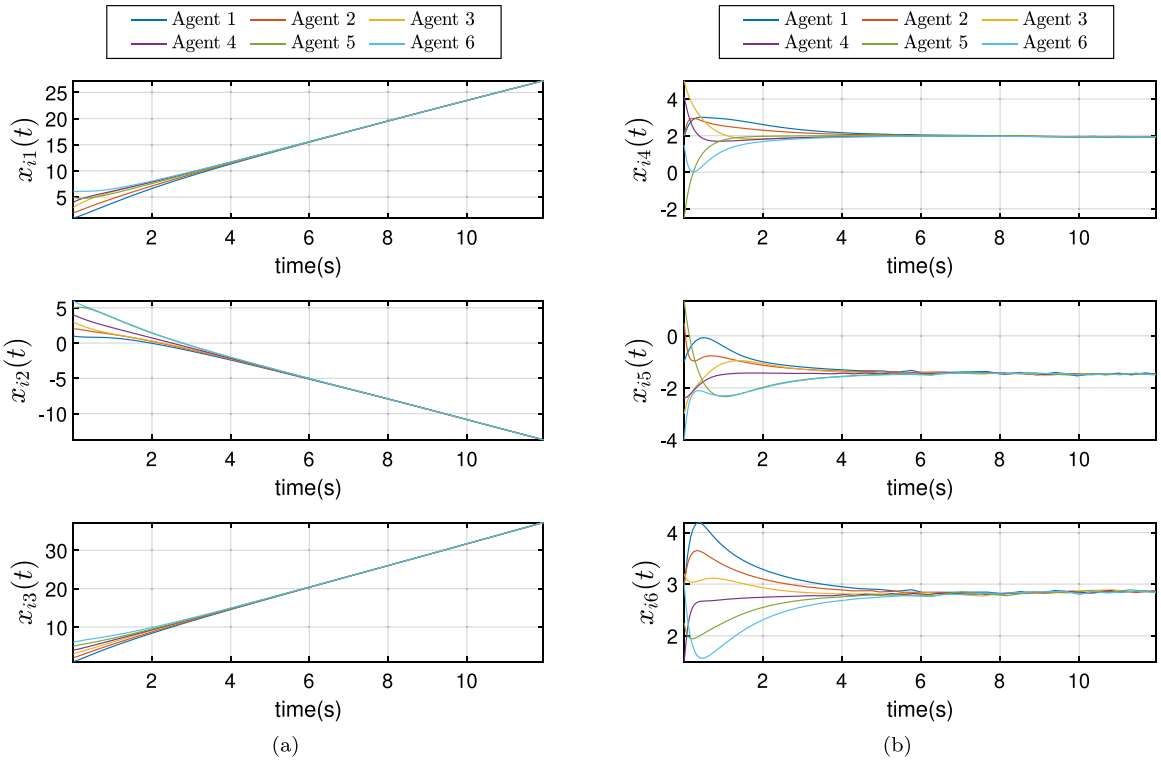

Fig. 8. (a). Trajectory curves of agents' position state of Example II. (b). Trajectory curves of agents' velocity state of Example II.

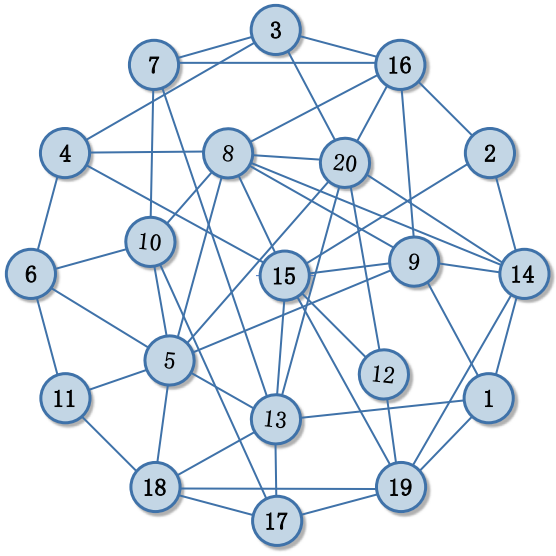

Fig. 9. The topology among 20 agents of Example III.

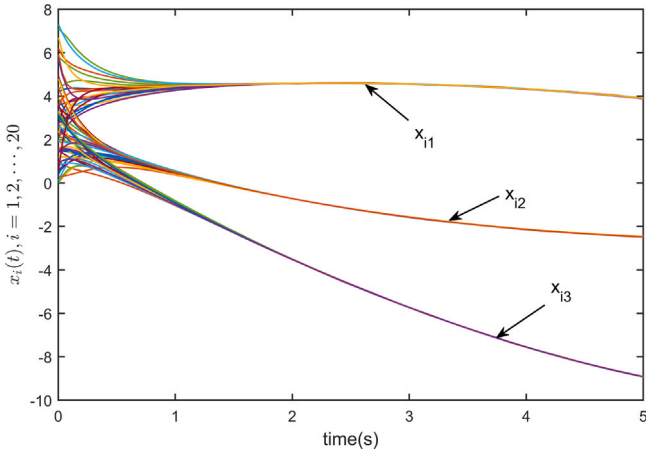

Fig. 10. Trajectory curves of agents' velocity state of Example III.

matrices A and B are as follows:

$$A = \begin{pmatrix} -0.4639 & -0.2629 & 0.0400 \\ -0.2112 & 0.1067 & 0.1647 \\ -0.0418 & -0.6390 & -0.1428 \end{pmatrix}, B = \begin{pmatrix} 2 & 0 & 0 \\ 0 & 2 & 0 \\ 0 & 0 & 2 \end{pmatrix}.$$

By setting $R = 1$, we can solve ARE (11) and yields that $\lambda = 0.6469$ and

$$K = \begin{pmatrix} 0.5176 & -0.0678 & -0.0038 \\ -0.0678 & 0.7049 & -0.0656 \\ -0.0038 & -0.0656 & 0.5935 \end{pmatrix},$$

The minimum and maximum detection intervals are set $h_m = 0.02s$ and $h_M = 0.04s$ respectively. With the initial conditions as [28], the time evolutions of agents' states are depicted in Fig. 10, which implies that in the context of an expanding number of nodes within MASs, the proposed protocol still remains capable of achieving consensus. This can be attributed to the variable and asynchronous detection intervals introduced in our proposed approach. By circumventing the synchronization challenges associated with periodic detection, ASDETC may be more suitable in large-scale systems.

5. Conclusion

This brief provides a new event-triggered consensus controller for MASs via the adaptive sampling detection. Several sufficient conditions have been established to ensure consensus is reached in MASs under directed and switching topologies, while the Zeno phenomenon is entirely avoided. This solution provides less energy consumption

compared to existing dynamic event-triggered protocols. In the future, a dynamic event-triggered consensus control method based on adaptive sampling for heterogeneous MASs and under network disturbances will be considered.

CRediT authorship contribution statement

Yiming Wu: Writing – review & editing, Supervision. **Nan Tang:** Writing – original draft. **Xiaozhen Pan:** Writing – review & editing, Supervision. **Ming Xu:** Funding acquisition. **Shuai Liu:** Formal analysis.

Declaration of competing interest

The authors declare that they have no known competing financial interests or personal relationships that could have appeared to influence the work reported in this paper.

Acknowledgment

This work was supported by Zhejiang Provincial Public Welfare Research Project of China under Grant LGF21F020011.

Data availability

No data was used for the research described in the article.

References

[1] R. Olfati-Saber, R.M. Murray, Consensus problems in networks of agents with switching topology and time-delays, IEEE Trans. Autom. Control 49 (9) (2004) 1520–1533.
[2] L. Zhang, S. Liu, Distributed average consensus of stochastic singularly perturbed systems, IEEE Trans. Control. Netw. Syst. 10 (4) (2023) 1913–1924.
[3] L. Zhou, J. Wang, M. Ye, B.-L. Zhang, Y. Zheng, Consensus of hybrid behavior for graphical coordination games, IEEE Trans. Circ. Syst. II: Express Briefs 70 (8) (2023) 3009–3013.
[4] D.V. Dimarogonas, E. Frazzoli, K.H. Johansson, Distributed event-triggered control for multi-agent systems, IEEE Trans. Autom. Control 57 (5) (2011) 1291–1297.
[5] G. Guo, L. Ding, Q.-L. Han, A distributed event-triggered transmission strategy for sampled-data consensus of multi-agent systems, Automatica 50 (5) (2014) 1489–1496.
[6] Z. Gu, Y. Fan, X. Sun, X. Xie, C.K. Ahn, Event-based two-step transmission mechanism for the stabilization of networked T–s fuzzy systems with random uncertainties, IEEE Trans. Cybern. 54 (2) (2024) 1283–1293.
[7] Z. Gu, X. Huang, X. Sun, X. Xie, J.H. Park, Memory-event-triggered tracking control for intelligent vehicle transportation systems: A leader-following approach, IEEE Trans. Intell. Transp. Syst. 25 (5) (2024) 4021–4031.
[8] B. Cheng, Z. Li, Fully distributed event-triggered protocols for linear multiagent networks, IEEE Trans. Autom. Control 64 (4) (2018) 1655–1662.
[9] A. Girard, Dynamic triggering mechanisms for event-triggered control, IEEE Trans. Autom. Control 60 (7) (2014) 1992–1997.
[10] E. Bernuau, E. Moulay, P. Coirault, F. Isfoula, Practical consensus of homogeneous sampled-data multiagent systems, IEEE Trans. Autom. Control 64 (11) (2019) 4691–4697.
[11] Y. Wu, H. Su, P. Shi, Z. Shu, Z.-G. Wu, Consensus of multiagent systems using aperiodic sampled-data control, IEEE Trans. Cybern. 46 (9) (2015) 2132–2143.
[12] W. He, B. Zhang, Q.-L. Han, F. Qian, J. Kurths, J. Cao, Leader-following consensus of nonlinear multiagent systems with stochastic sampling, IEEE Trans. Cybern. 47 (2) (2016) 327–338.
[13] W. Liu, J. Huang, Leader-following consensus for linear multiagent systems via asynchronous sampled-data control, IEEE Trans. Autom. Control 65 (7) (2019) 3215–3222.
[14] G. Zhao, C. Hua, Leader-following consensus of multiagent systems via asynchronous sampled-data control: A hybrid system approach, IEEE Trans. Autom. Control 67 (5) (2021) 2568–2575.
[15] Y. Shi, Q. Hu, X. Shao, Y. Shi, Adaptive neural coordinated control for multiple Euler-Lagrange systems with periodic event-triggered sampling, IEEE Trans. Neural Netw. Learn. Syst. 34 (11) (2023) 8791–8801, http://dx.doi.org/10.1109/TNNLS.2022.3153077.
[16] N. Lin, Q. Ling, Dynamic periodic event-triggered consensus protocols for linear multiagent systems with network delay, IEEE Syst. J. 17 (1) (2023) 1204–1215, http://dx.doi.org/10.1109/JSYST.2022.3173939.
[17] M.H. Dhullipalla, H. Yu, T. Chen, A framework for distributed control via dynamic periodic event-triggering mechanisms, Automatica 146 (2022) 110548.
[18] H. Zhu, J. Liu, Z. Zhang, S. Zhang, F. Qu, X. Liu, H_∞ consensus of multi-agent systems under hybrid cyber attacks via a sampled-data-based dynamic event-triggered resilient consensus protocol, J. Franklin Inst. 360 (13) (2023) 9924–9949.
[19] T. Xu, Y. Niu, Z. Cao, Sliding mode control for Markovian jump systems with stochastic-sampling-based event-triggered strategy, IEEE Trans. Autom. Control. 69 (11) (2024) 8064–8071, http://dx.doi.org/10.1109/TAC.2024.3407826.
[20] Z. Cheng, H. Ren, Y. Xiao, Y. Qiu, Aperiodic sampling event-triggered consensus control for multi-agent systems, in: 2020 7th International Conference on Information, Cybernetics, and Computational Social Systems, ICCSS, IEEE, 2020, pp. 260–265.
[21] Z. Sheng, S. Xu, An aperiodic-sampling-dependent event-triggered control strategy for interval type-2 fuzzy systems: New communication scheme and discontinuous functional, IEEE Trans. Cybern. 54 (11) (2024) 6436–6447, http://dx.doi.org/10.1109/TCYB.2024.3432909.
[22] X. Kong, Y. Wang, A detection-interval-varying event-triggering mechanism for multi-agent systems with disturbances, in: 2021 CAA Symposium on Fault Detection, Supervision, and Safety for Technical Processes, SAFEPROCESS, IEEE, 2021, pp. 1–6.
[23] V. Kucera, A contribution to matrix quadratic equations, IEEE Trans. Autom. Control. 17 (3) (1972) 344–347.
[24] X. Meng, T. Chen, Event based agreement protocols for multi-agent networks, Autom. 49 (7) (2013) 2125–2132.
[25] W. Hu, C. Yang, T. Huang, W. Gui, A distributed dynamic event-triggered control approach to consensus of linear multiagent systems with directed networks, IEEE Trans. Cybern. 50 (2) (2018) 869–874.
[26] W. Lu, T. Chen, New approach to synchronization analysis of linearly coupled ordinary differential systems, Phys. D: Nonlinear Phenom. 213 (2) (2006) 214–230.
[27] W. Yu, G. Chen, M. Cao, J. Kurths, Second-order consensus for multiagent systems with directed topologies and nonlinear dynamics, IEEE Trans. Syst. Man, Cybern. Part B (Cybernetics) 40 (3) (2010) 881–891.
[28] W. He, Z. Mo, Secure event-triggered consensus control of linear multiagent systems subject to sequential scaling attacks, IEEE Trans. Cybern. 52 (10) (2022) 10314–10327.